



Exploring the mass assembly of the early-type disc galaxy NGC 3115 with MUSE

A. Guérou^{1,2,3,*}, E. Emsellem^{3,4}, D. Krajnović⁵, R. M. McDermid^{6,7}, T. Contini^{1,2}, and P. M. Weilbacher⁵

¹ IRAP, Institut de Recherche en Astrophysique et Planétologie, CNRS, 14, avenue Edouard Belin, F-31400 Toulouse, France

² Université de Toulouse, UPS-OMP, Toulouse, France

³ European Southern Observatory, Karl-Schwarzschild-Str. 2, D-85748 Garching, Germany e-mail: aguero@eso.org

⁴ Université Lyon 1, Observatoire de Lyon, Centre de Recherche Astrophysique de Lyon and Ecole Normale Supérieure de Lyon, 9 avenue Charles André, F-69230 Saint-Genis Laval, France

⁵ Leibniz-Institut für Astrophysik Potsdam (AIP), An der Sternwarte 16, D-14482 Potsdam, Germany

⁶ Department of Physics and Astronomy, Macquarie University, Sydney NSW 2109, Australia

⁷ Australian Astronomical Observatory, PO Box 915, Sydney NSW 1670, Australia

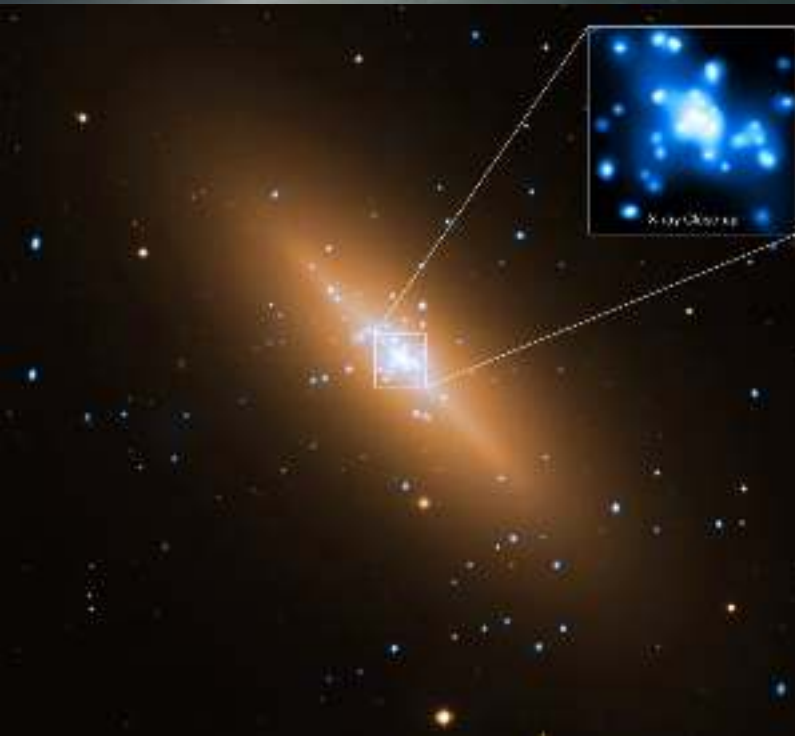
Received ... ; accepted ...

ABSTRACT

We present MUSE integral field spectroscopic data of the S0 galaxy NGC 3115 obtained during the instrument commissioning at the ESO Very Large Telescope (VLT). We analyse the galaxy stellar kinematics and stellar populations and present two dimensional maps of their associated quantities. We thus illustrate the capacity of MUSE to map extra-galactic sources to large radii in an efficient manner, i.e., $\sim 4 R_e$, and provide relevant constraints on its mass assembly. We probe the well known set of substructures of NGC 3115 (its nuclear disc, stellar rings, outer kpc-scale stellar disc and spheroid) and show their individual associated signatures in the MUSE stellar kinematics and stellar populations maps. In particular, we confirm that NGC 3115 has a thin fast rotating stellar disc embedded in a fast rotating spheroid, and that these two structures show clear differences in their stellar age and metallicity properties. We emphasise an observed correlation between the radial stellar velocity, V , and the Gauss-Hermite moment, h_3 , creating a “butterfly” shape in the central $15''$ of the h_3 map. We further detect the previously reported weak spiral and ring-like structures, and find evidence that these features can be associated with regions of younger mean stellar ages. We provide tentative evidence for the presence of a bar, despite the fact that the V - h_3 correlation can be reproduced by a simple axisymmetric dynamical model. Finally, we present a reconstruction of the two dimensional star formation history of NGC 3115 and find that most of its current stellar mass was formed at early epochs (>12 Gyr ago), while star formation continued in the outer (kpc-scale) stellar disc until recently. Since $z \sim 2$, and within $\sim 4 R_e$, we suggest that NGC 3115 has been mainly shaped by secular processes.



NGC 3115



30''

- NGC3115 is the closest S0 galaxy to the Milky Way ($d = 9.8\text{Mpc}$, Cantiello et al. 2014), with a subsequently large apparent diameter ($\mu_B = 25 \text{ mag.arcsec}^2 \sim 8'$).
- It is bright and almost edge-on ($i = 86^\circ$, Capaccioli et al. 1987) with very little dust and gas (Li et al. 2011; Li & Wang 2013).
- It has a smooth surface brightness distribution, making it ideal to test the “spectro-imager” and mosaicing abilities of MUSE.
- NGC3115 is also a very interesting object with a complex set of substructures, including
 - a nuclear disc and an outer (kpc-scale) disc (Capaccioli et al. 1987; Nieto et al. 1991; Scorza & Bender 1995; Lauer et al. 1995; Emsellem et al. 1999),
 - possible rings and spirals (Norris et al. 2006; Michard 2007; Savorgnan & Graham 2016),
 - a rapidly rotating spheroid (Arnold et al. 2011, 2014),
 - a large globular clusters system exhibiting a clear bi-modality (Kuntschner et al. 2002; Brodie et al. 2012; Jennings et al. 2014; Cantiello et al. 2014),
 - a central super-massive black hole (Kormendy & Richstone 1992; Kormendy et al. 1996; Emsellem et al. 1999) and
 - a few X-ray sources (Wong et al. 2011; Wrobel & Nyland 2012).

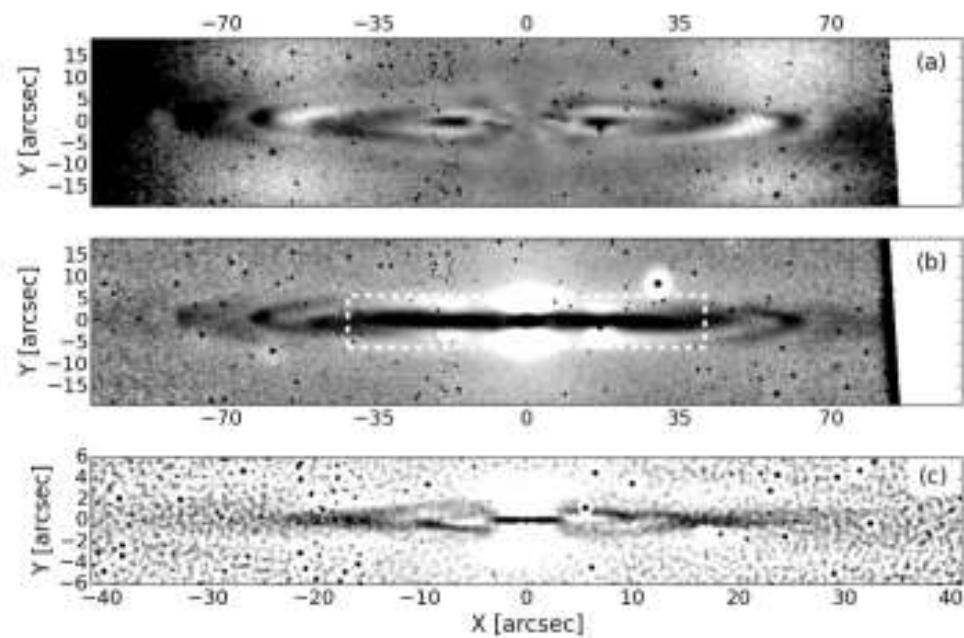
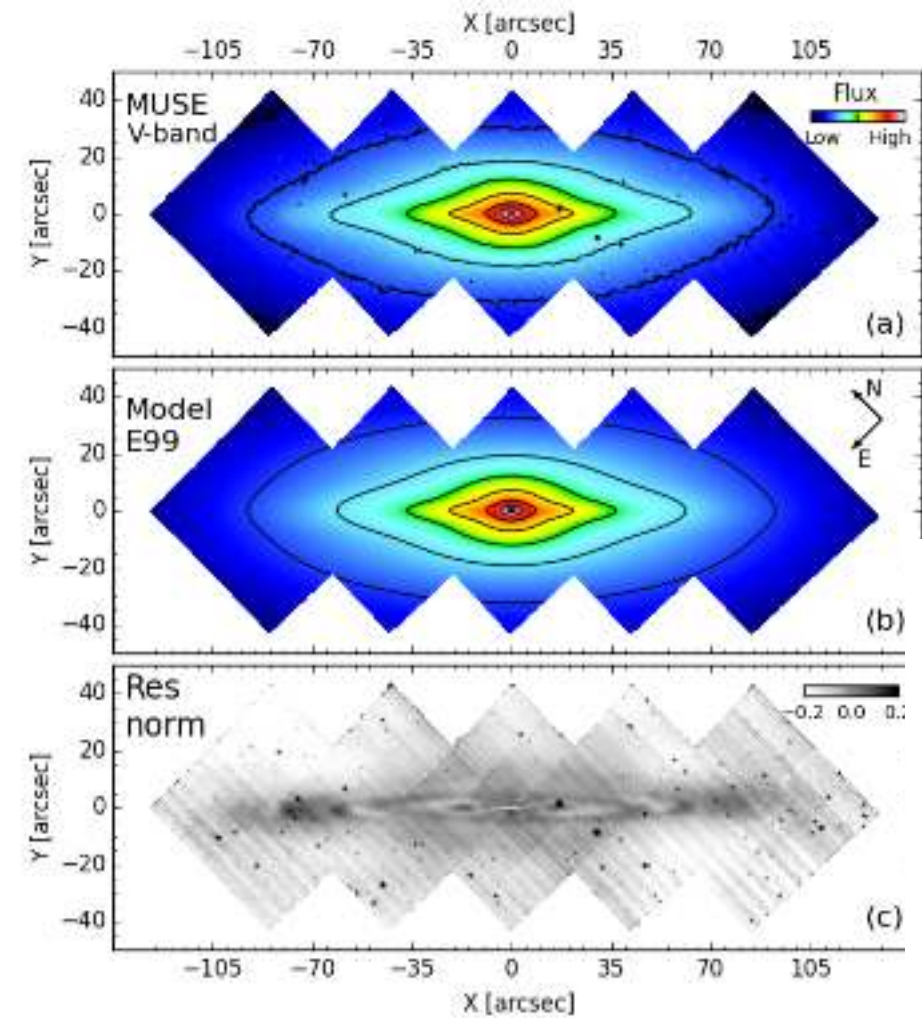


Fig. 11. (a): ACS/HST residuals after removal of the MGE photometric model (Emsellem et al. 1999); (b): Unsharp masking of the HST image; (c): Zoom corresponding to the dashed rectangle of the unsharp masking image (panel b).

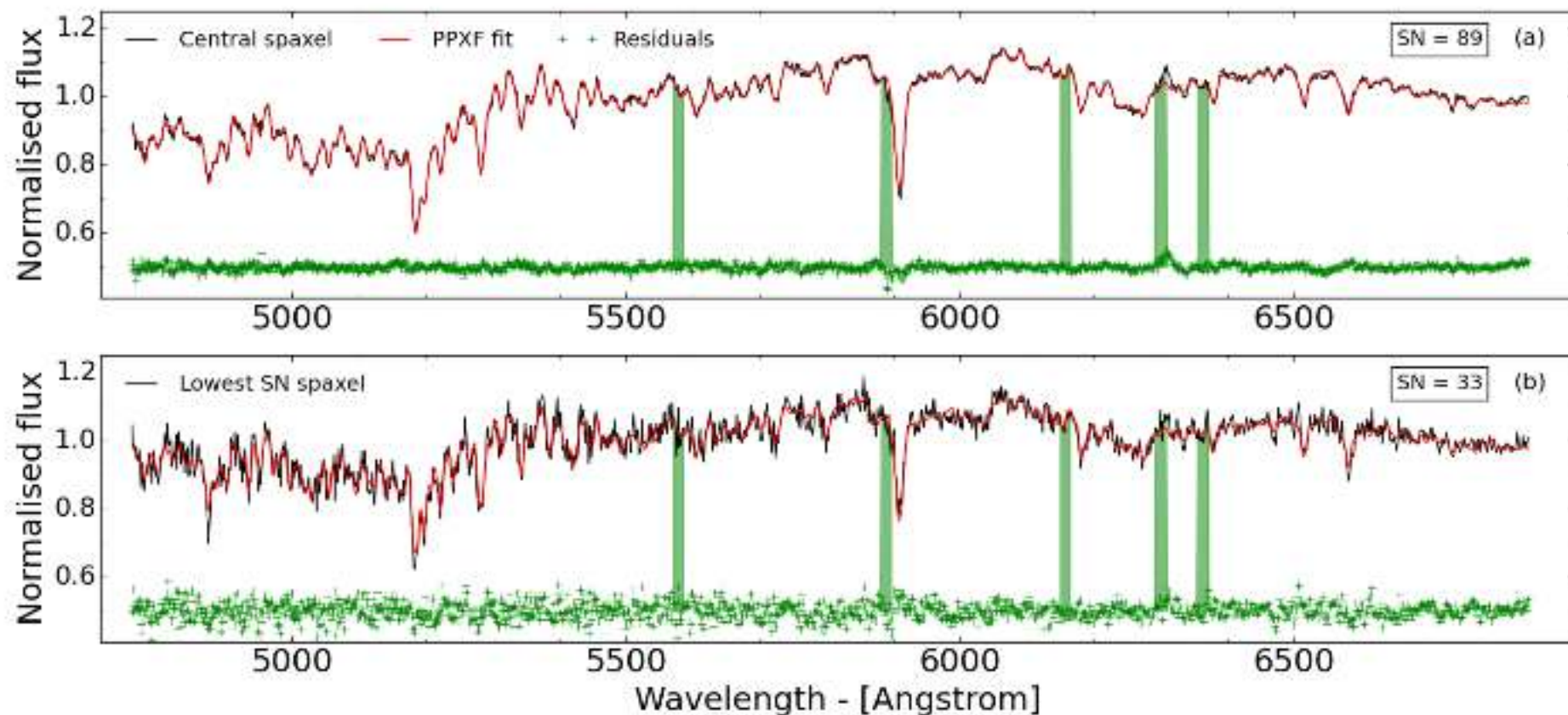
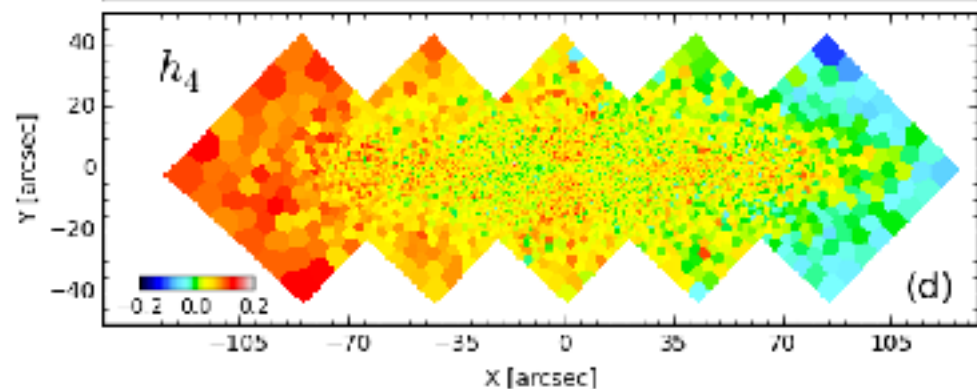
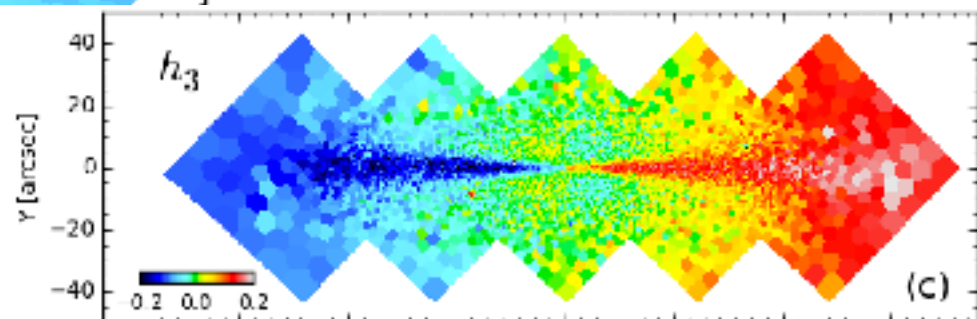
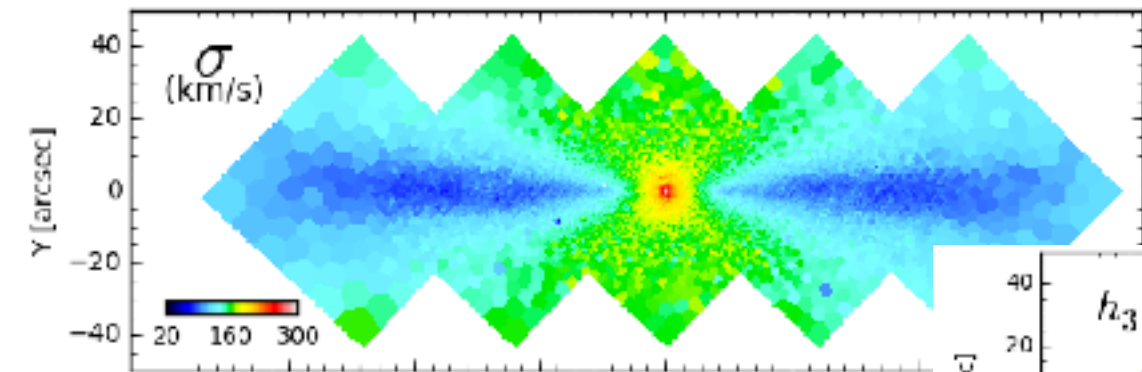
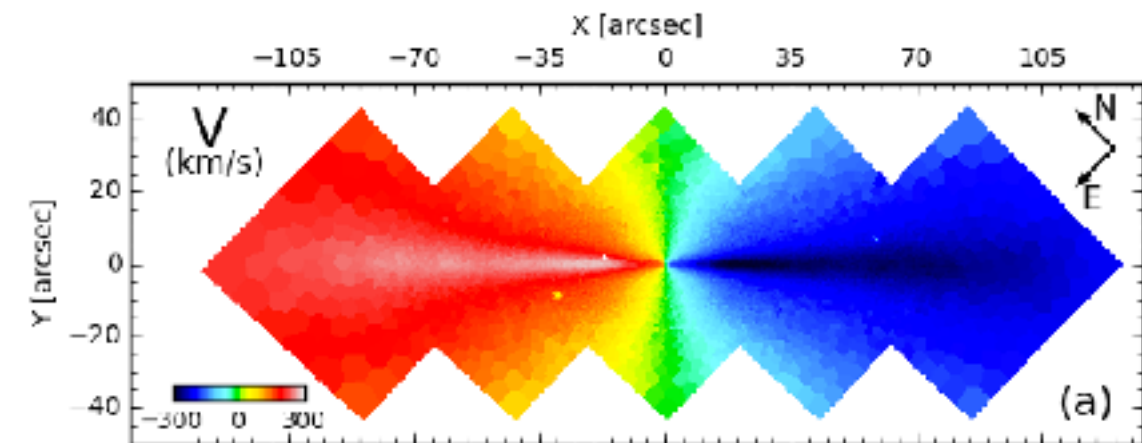
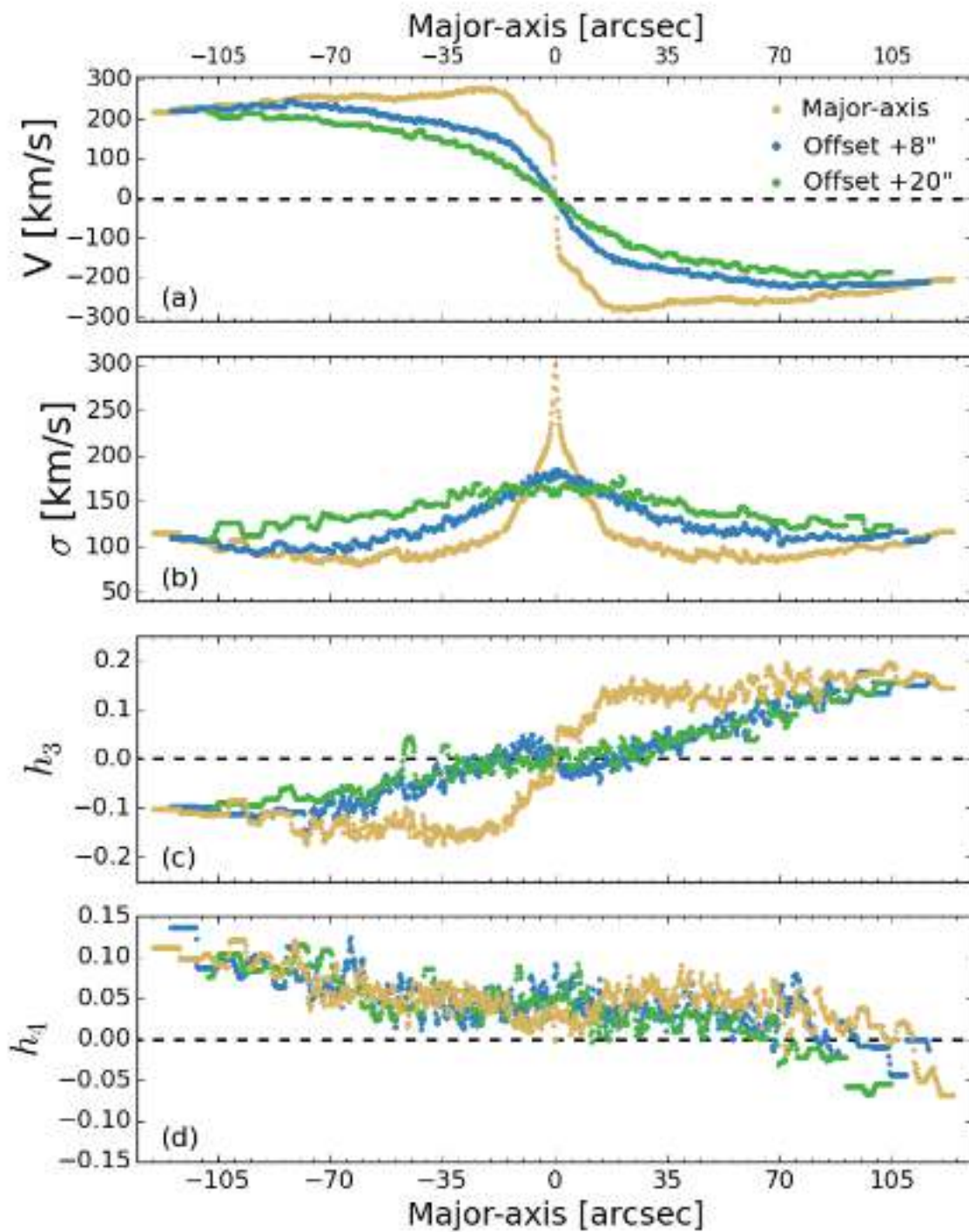


Fig. 2. Stellar kinematics fits: (a) of the central spaxel, and (b) the lowest S/N spectrum of our MUSE NGC 3115 data cube. The fits were performed with the pPXF software (Cappellari & Emsellem 2004) using the MILES stellar library (Sanchez-Blazquez et al. 2006; Falcón-Barroso et al. 2011), between 4760 – 6850 Å. The black lines show the MUSE spectra, the red lines the best fits, the shaded green areas are the wavelength ranges not fitted (i.e., corresponding to the sky lines regions), and the green crosses show the fit residuals (shifted upwards by 0.5 along the y axis). The upper-right box in each panel indicates the respective S/N of the MUSE spectrum showed.





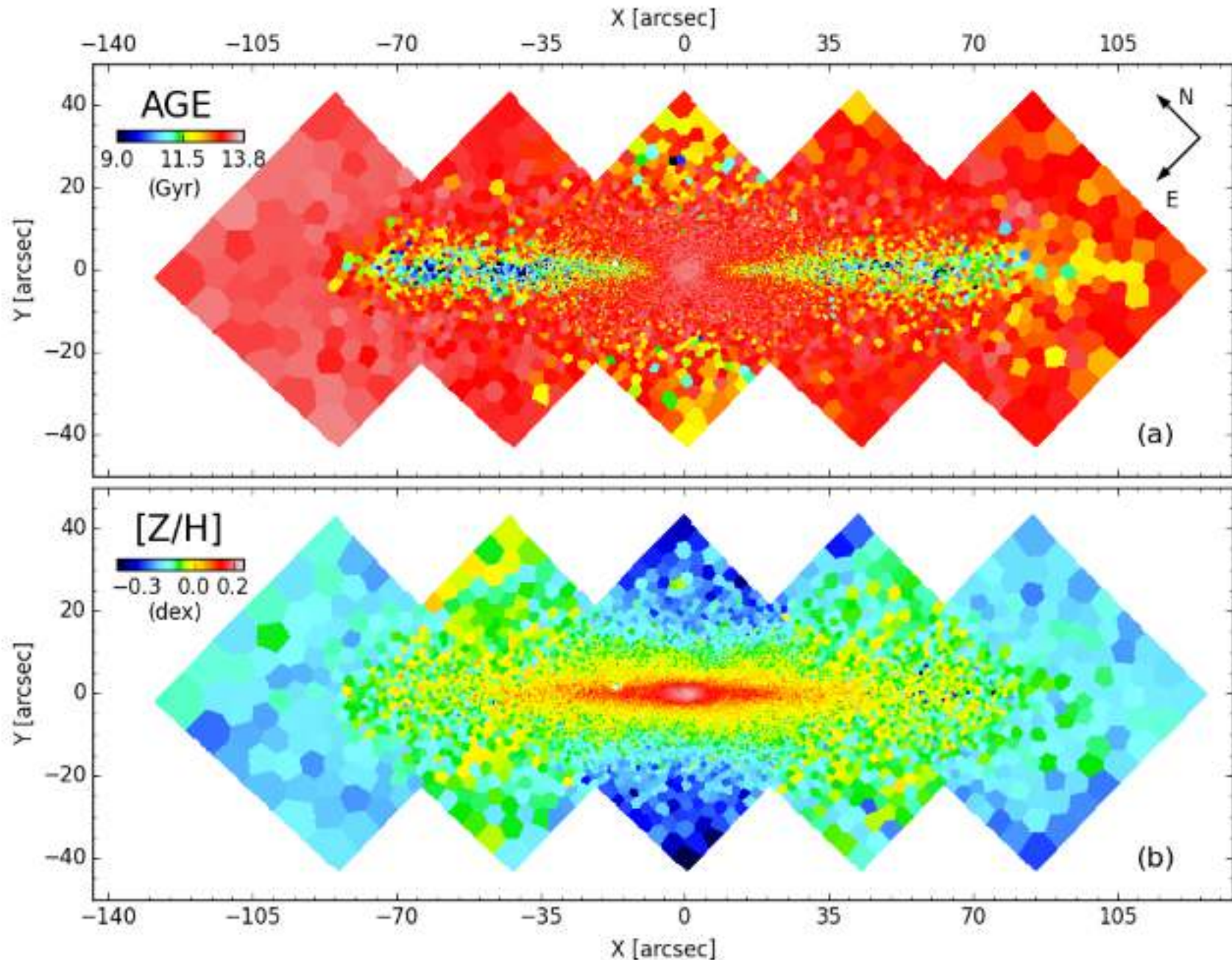


Fig. 5. Maps of the stellar population of NGC 3115 obtained through regularised full spectral fitting: (a) Mass weighted age ; and (b) mass weighted metallicity, $[Z/H]$. The color code for each panel is indicated on its top left corner. We observe a clear distinction of age between the disc and the spheroid component of NGC 3115, as well as a clear metallicity gradient along the major- and minor-axis of the stellar disc.

Stellar mass fraction - (Age)

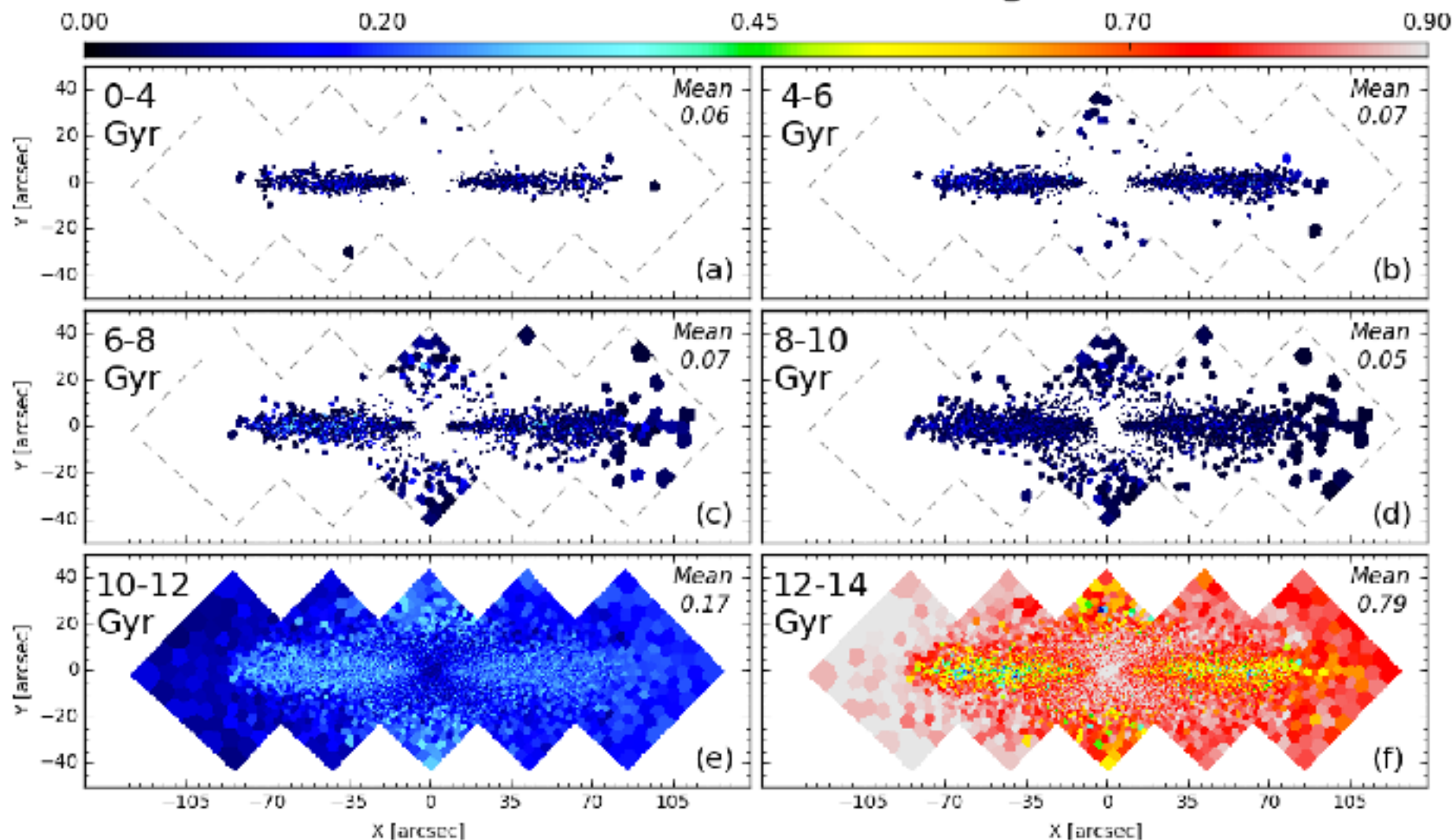


Fig. 7. Stellar mass fraction maps of NGC 3115, in six bins of age, obtained by projecting the stellar models weighting distribution solution, obtained with pPXF, onto the grid parameters (Age, $[Z/H]$). For each panel, the age bin limits are indicated on its top-left corner, the mean stellar mass fraction on its top-right corner, and the color scheme by the color bar at the top of the figure. Spaxels containing a stellar mass fraction lower than 0.03 are masked, considered below our uncertainties. The galaxy orientation is similar to Fig. 3. The extended star formation history of the outer disc component is clearly visible in the first four panels (a to d), whereas the stars present in the spheroid were formed early (age ≥ 10 Gyr), with more than 85% of its stellar mass formed between 12 – 14 Gyr (panels e and f).

Stellar mass [M_{\odot}] - (Age)

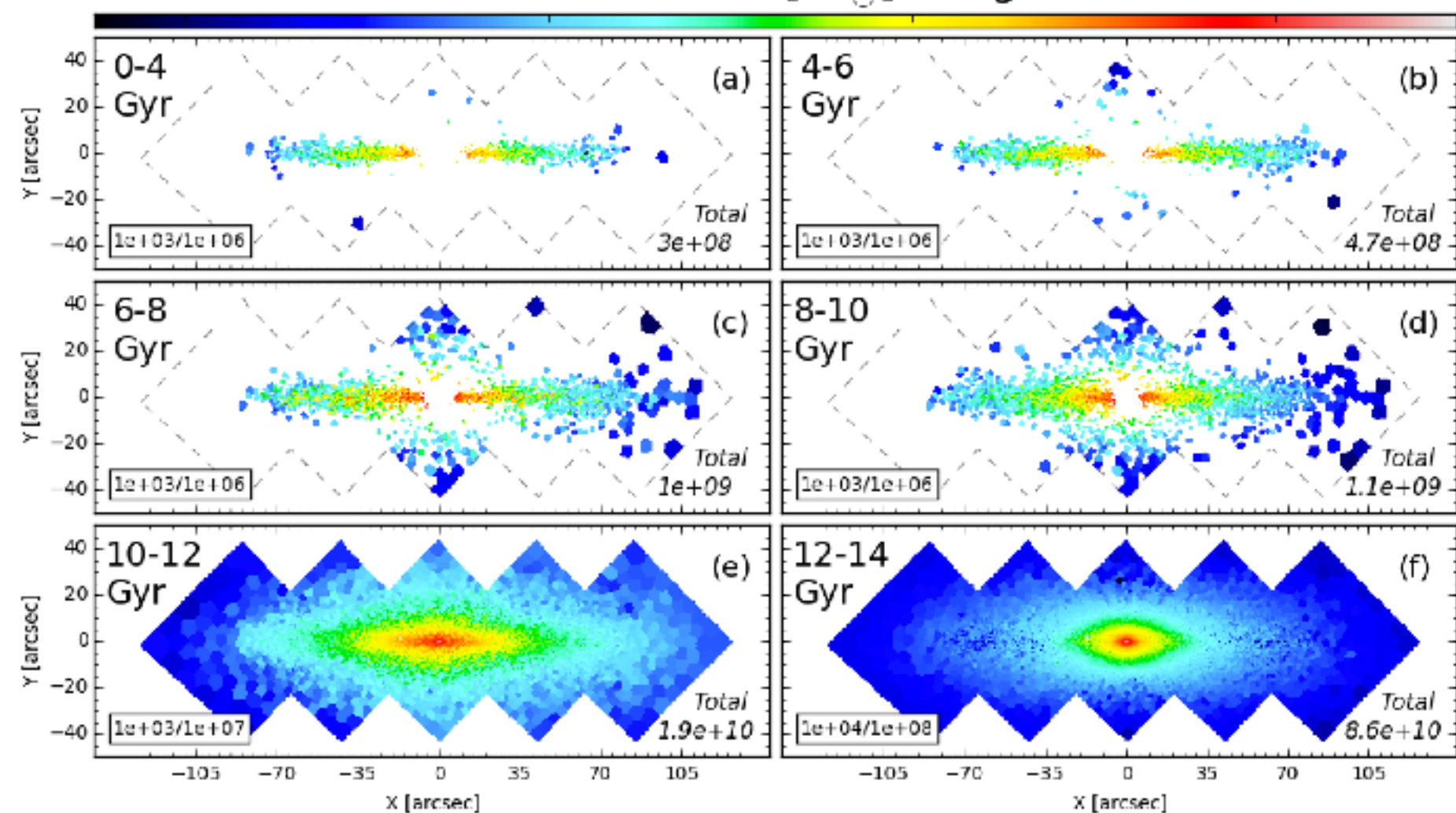


Fig. 8. Stellar mass maps of NGC 3115, in six bins of age, as in Figure 7. These maps show the present day stellar mass distribution as a function of its mass-weighted age. For each panel, the total stellar mass per bin of age (in solar mass) is indicated at its bottom-right corner, and the color scheme limits (corresponding to the color bar at the top) are indicated on its bottom-left corner, and vary from one another. The noticeable change in the shape of the iso-mass contours between 10 – 12 Gyr and 12 – 14 Gyr, from rather flat to more spheroidal, suggests a more dissipative mass assembly at early epoch (age > 12 Gyr) possibly from a major merger. Panels (a) to (c) suggest that extended star formation occurred in-situ in the disc component of NGC 3115.

Stellar mass fraction - ($[Z/H]$)

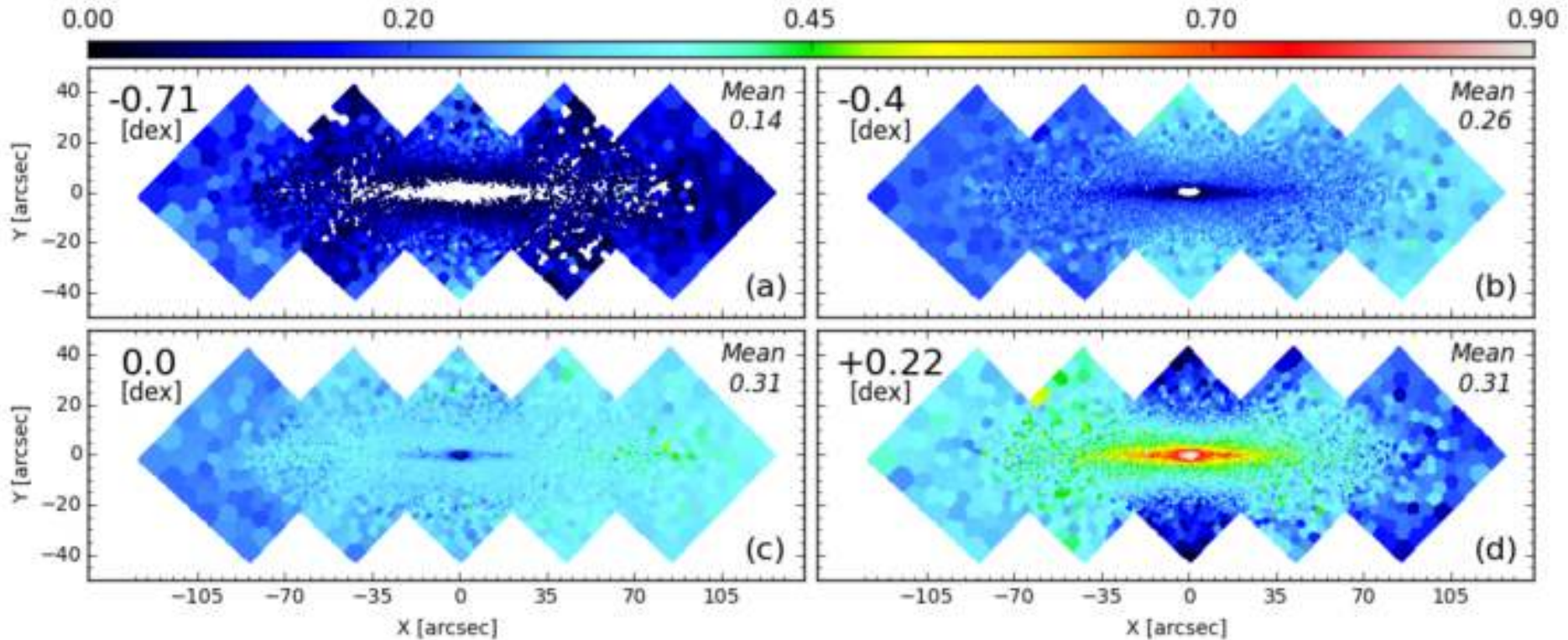


Fig. 9. Stellar mass fraction maps of NGC 3115, in four bins of metallicity, marginalised over age. For each panel, the metallicity bin limits are indicated on its top-left corner, the mean stellar mass fraction on its top-right corner, and the color scheme by the color bar at the top of the figure. Spaxels containing a stellar mass fraction lower than 0.03 are masked, considered below our uncertainties. The galaxy orientation is the same as Fig. 3. It is remarkable that the central 10'' where the inner disc resides, are made of only metal-rich stars (panel *d*). The disc component has very little metal-poor stars (panels *a* and *b*), and the spheroid of NGC 3115 has a flat distribution over the four metallicity bins, from metal-rich to metal-poor.

Stellar mass fraction - (Age & [Z/H])

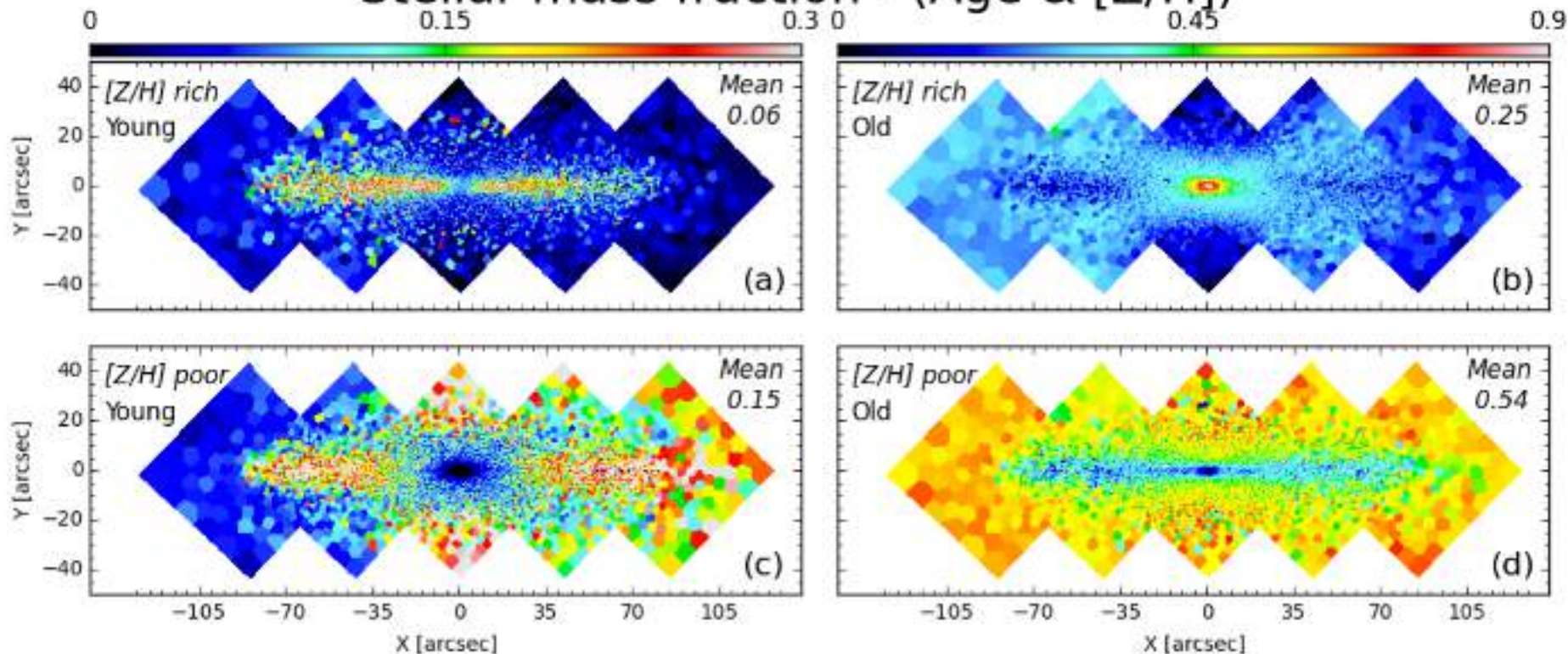
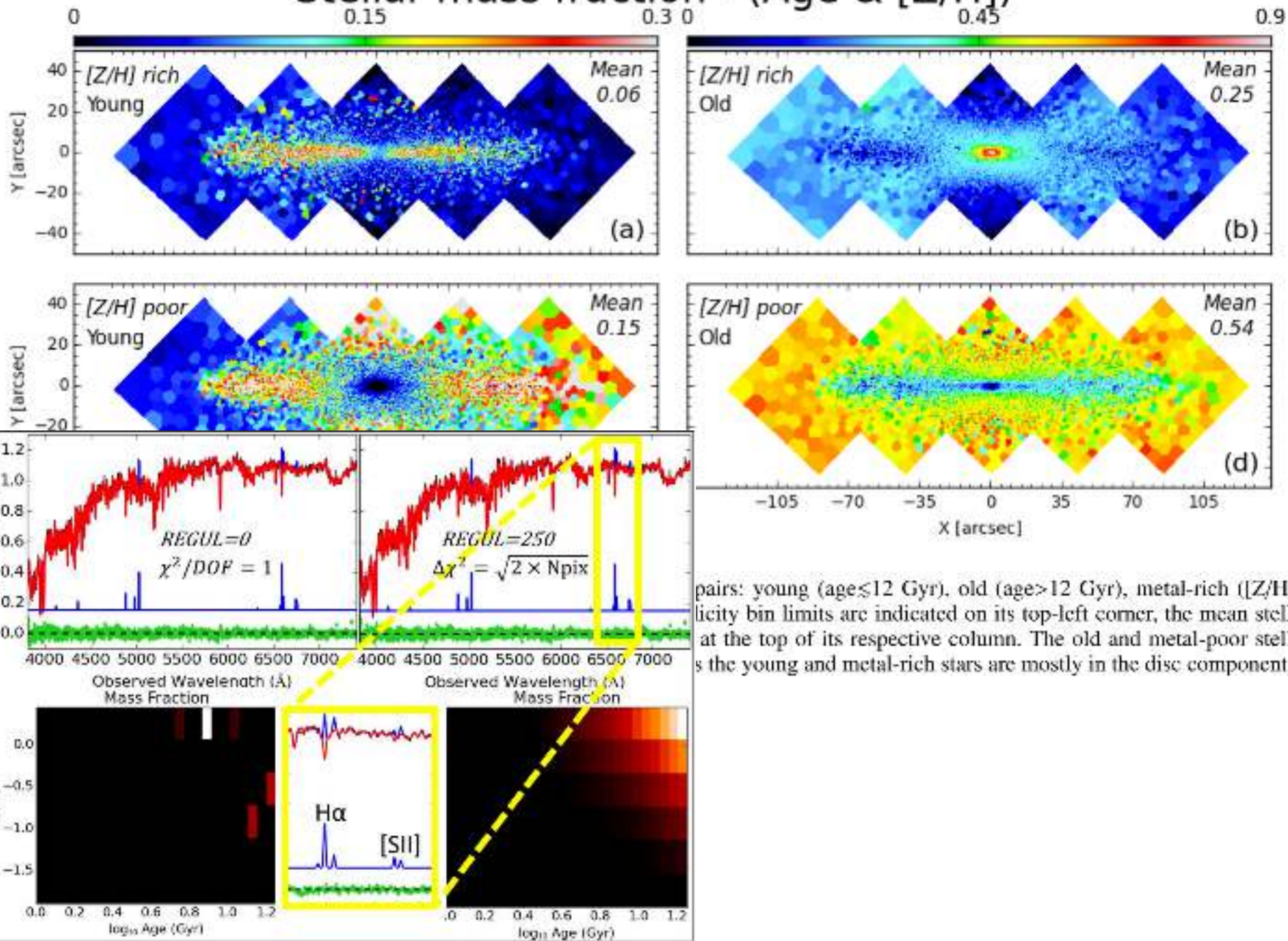


Fig. 10. Stellar mass fraction of NGC 3115 in four bins of age/metallicity pairs: young ($\text{age} \leq 12$ Gyr), old ($\text{age} > 12$ Gyr), metal-rich ($[Z/H] = 0.2$ dex) and metal-poor ($[Z/H] < 0.2$ dex). For each panel, the age and metallicity bin limits are indicated on its top-left corner, the mean stellar mass fraction on its top-right corner, and the color scheme by the color bar at the top of its respective column. The old and metal-poor stellar population of NGC 3115 is mostly located in its spheroid component, whereas the young and metal-rich stars are mostly in the disc component.

Stellar mass fraction - (Age & [Z/H])



pairs: young (age ≤ 12 Gyr), old (age > 12 Gyr), metal-rich ([Z/H] = ...), metal-poor ([Z/H] = ...). The young and metal-rich stars are mostly in the disc component.

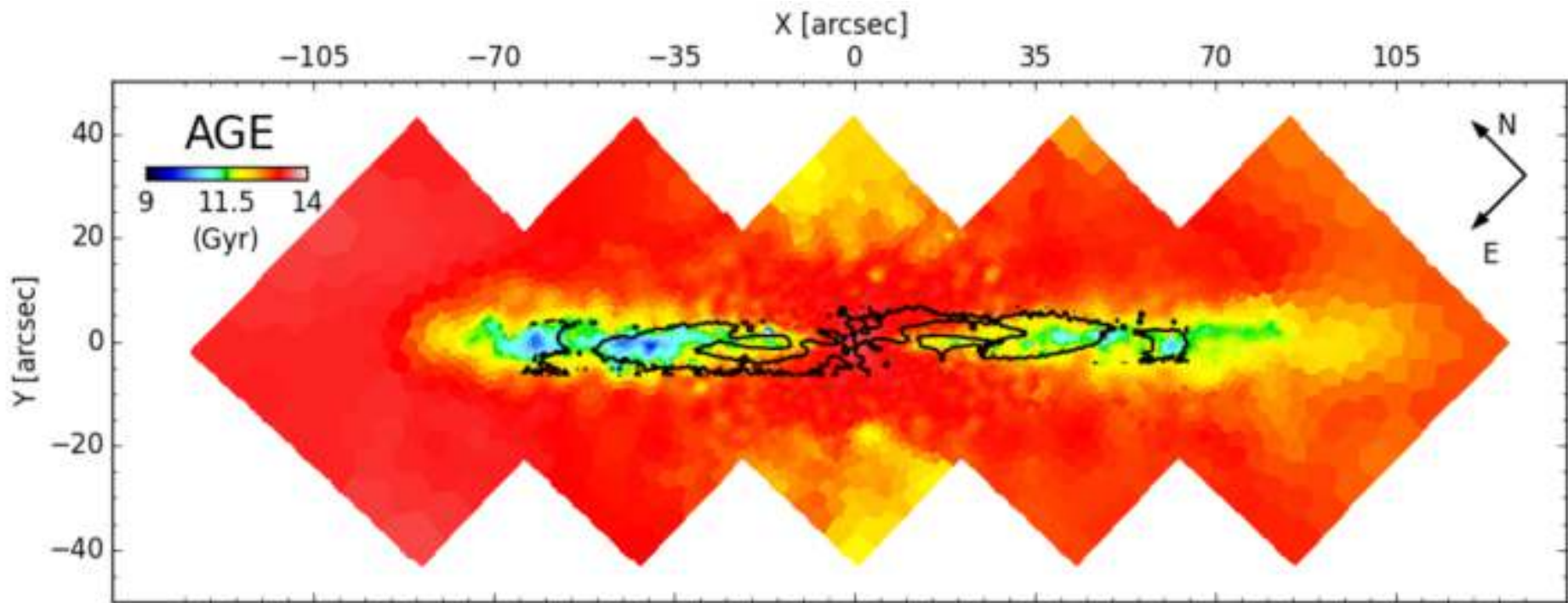


Fig. 12. Smoothed version of the stellar age map of NGC 3115, with the ACS/HST residuals contours over-plotted on top. We plotted only the zero-level contours corresponding to the potential spiral-arms in order to enlighten their boundaries. A clear spatial match is observed between the spiral-like residual structures and the youngest stellar population observed.

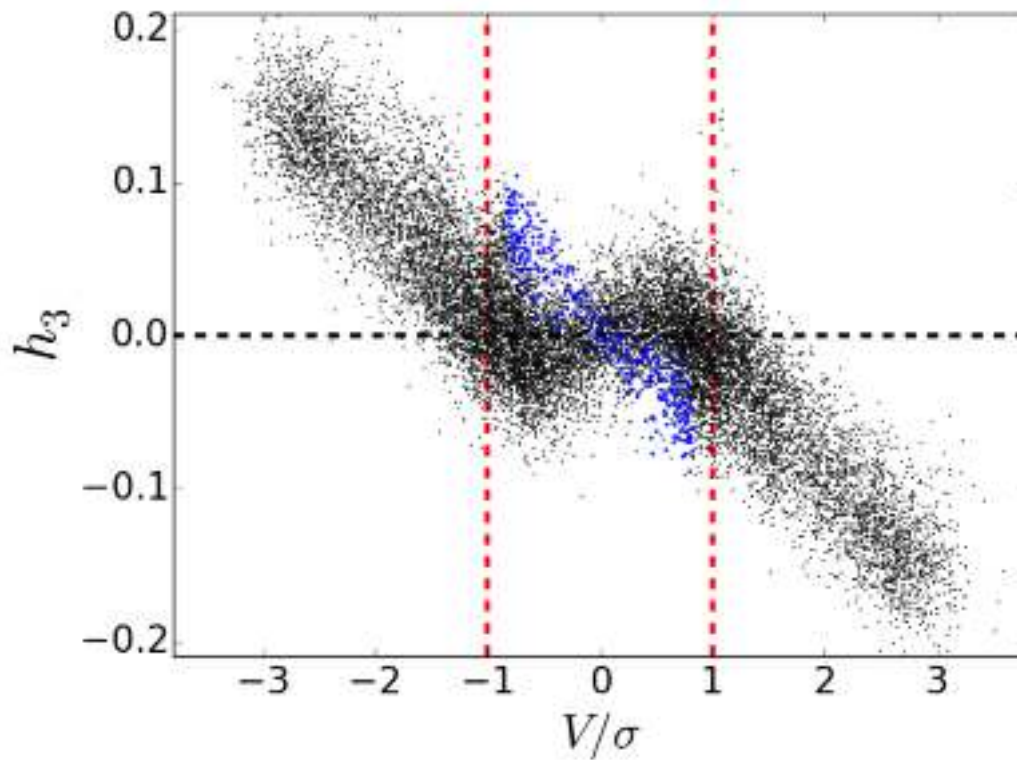


Fig. 13. Third Gauss-hermite moment, h_3 , versus V/σ for each spaxel of NGC 3115 MUSE cube. Blue dots represent the spaxels corresponding to the nuclear-disc (central $3'' \times 1''$) of NGC 3115.

Athanassoula & Bureau (1999) performed simulations of peanut-bulge dominated galaxies and concluded that in galaxies seen edge-on, strong bars may show up as:

- (i) a double maximum in the stellar rotation profile along the major-axis,
- (ii) (ii) a flat central stellar velocity dispersion profile (sometimes with a dip),
- (iii) (iii) an h_3 Gauss-Hermite moment correlated with the stellar radial velocity, V , over the bar length, and (iv) a h_3 Gauss-Hermite moment anti-correlated with V in the very centre where nuclear-discs are often present.

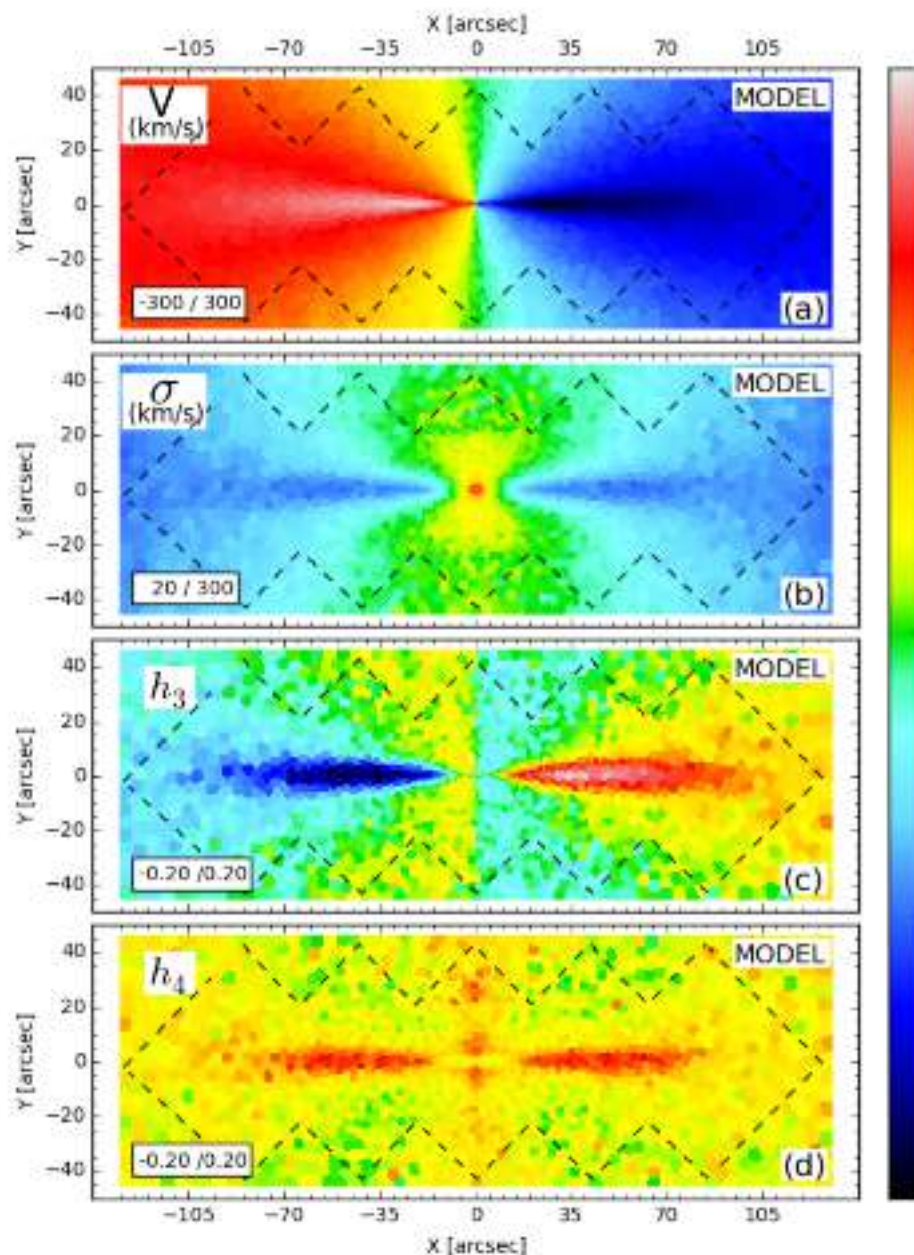
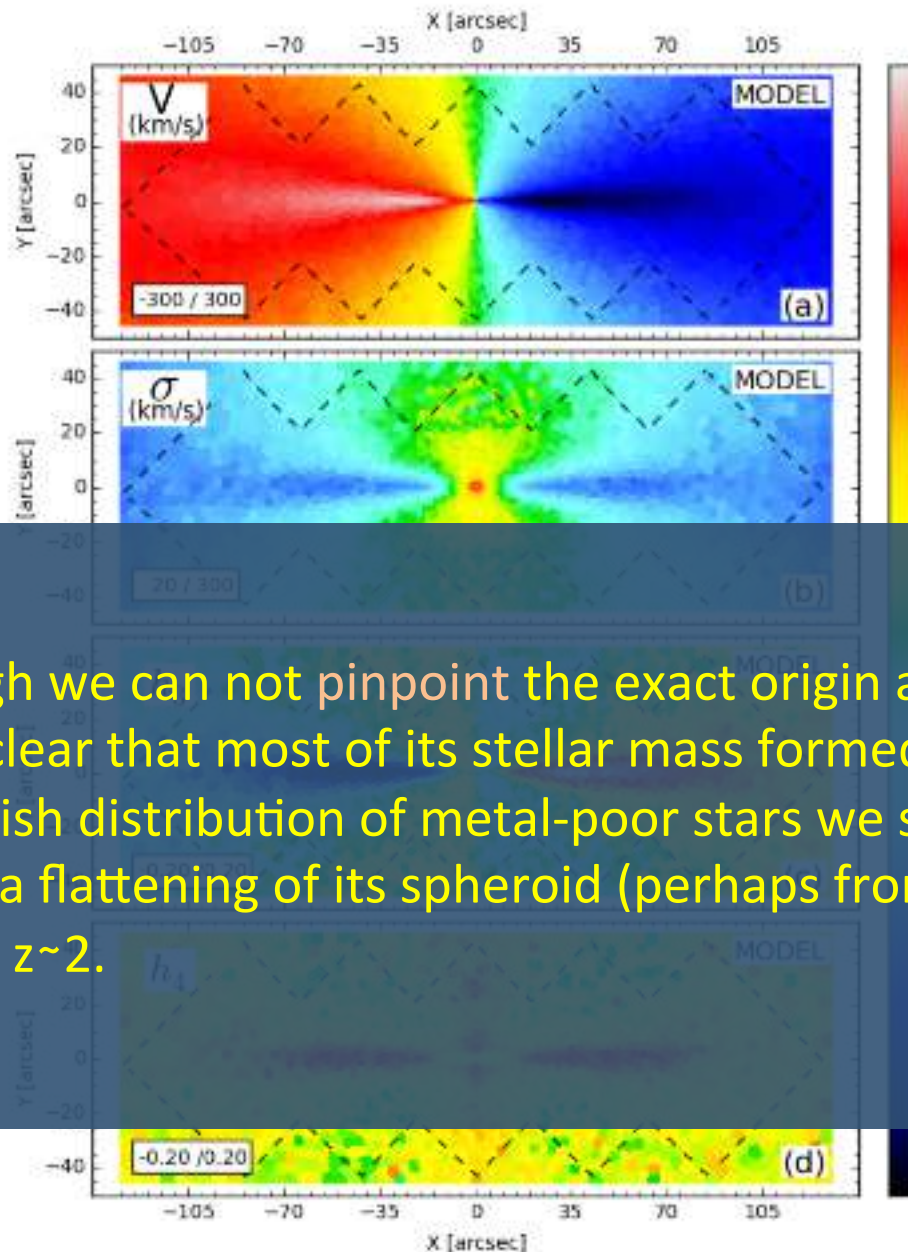


Fig. 14. As in Fig. 3, but for the dynamical model described in § 5.2. The dashed contours indicate the MUSE pointings coverage.



Finally, even though we can not pinpoint the exact origin and evolution history of NGC 3115, it is clear that most of its stellar mass formed at a redshift $z > 3$, creating the roundish distribution of metal-poor stars we see nowadays (within $4 R_e$), followed by a flattening of its spheroid (perhaps from a few merger events) by redshift $z \sim 2$.

Fig. 14. As in Fig. 3, but for the dynamical model described in § 5.2. The dashed contours indicate the MUSE pointings coverage.